Universal learning of nonlocal entropy via local correlations in non-equilibrium quantum states

Hao Liao, 1 Xuanqin Huang, 1 and Ping Wang 2, *

¹National Engineering Laboratory on Big Data System Computing Technology, Guangdong Province Engineering Center of China-made High Performance Data Computing System, College of Computer Science and Software Engineering, Shenzhen University, Shenzhen 518060, China ²Faculty of Arts and Sciences, Beijing Normal University, Zhuhai 519087, China (Dated: November 25, 2025)

Characterizing the nonlocal nature of quantum states is a central challenge in the practical application of large-scale quantum computation and simulation. Quantum mutual information (QMI), a fundamental nonlocal measure, plays a key role in quantifying entanglement and has become increasingly important in studying nonequilibrium quantum many-body phenomena, such as many-body localization and thermalization. However, experimental measurement of QMI remains extremely difficult, particularly for nonequilibrium states, which are more complex than ground states. In this Letter, we employ a multilayer perceptron (MLP) to establish a universal mapping between the QMI and local correlations only up to second order for nonequilibrium states generated by quenches in a one-dimensional disordered XXZ model. Our approach provides a practical method for experimentally extracting QMI, readily applicable in platforms such as superconducting qubits. Moreover, this work will establishes a general framework for reconstructing other nonlocal observables, including Fisher information and out-of-time-ordered correlators.

Introduction.—A fundamental distinction between quantum and classical mechanics lies in the non-local character of quantum states [1]. Their complete characterization generally requires an exponential number of local measurements, presenting a major challenge for quantum technologies [2]. A paradigmatic non-local measure is the quantum Rényi entropy (QRE), widely used in entanglement detection [3, 4], the characterization of phase transitions [5, 6], and studies of many-body physics [7]. Recent work has further revealed that non-equilibrium dynamics of the QRE [8] exhibits signatures of disorder-induced many-body localization (MBL) [9]. Accurate measurement of such non-local quantities is therefore crucial not only to quantum information theory, but also to understanding fundamental aspects of quantum non-equilibrium statistics [10–12], quantum chaos, and quantum gravity [13].

However, reconstructing non-local QRE in large-scale quantum systems remains challenging, as it generally requires quantum state tomography (OST), which becomes infeasible due to the exponential growth of Hilbert space dimension and measurement overhead. Although QRE has been measured in specific systems where multiple copies of a many-body state can be prepared and interfered [10, 12, 14, 15], its efficient measurement in generic, large-scale systems remains an open problem. Several approaches have recently been proposed to overcome this fundamental scaling issue, including randomized measurements [16, 17], matrix product state tomography [18], neural network quantum states [19–21], quantum neural networks [22], many-body interference [10], machine learning techniques [23, 24], and classical shadows [25]. These methods aim to predict non-local observables using data that scale polynomially with system size [23, 24]. Nevertheless, efficient and general reconstruction of QRE continues to pose significant challenges due to various method-specific limitations.

In this Letter, we employ a multilayer perceptron (MLP) to learn a universal function for predicting OMI in quench dynamics—a quantity derived from quantum Rényi entropy using only correlations with orders less than two, without resorting to OST. In contrast to the classical shadow method, randomized measurements and multi-task networks, which rely on the complete set of measurement outcomes [16, 17, 25] or short-range data[23, 24], we instead construct a mapping between the quantum mutual information and a substantially more compact and experimentally accessible data set. This approach is motivated by two key insights: (i) measurements of second-order correlations are significantly more efficient than those of higher-order correlations, which suffer from reduced signal-to-noise ratios and increased experimental overhead, even though higher-order measurements are feasible in certain systems [26]; (ii) although QMI of a nondegenerate ground state can be determined from second-order correlations alone [24, 27, 28], it remains unclear whether non-equilibrium states in closed quantum many-body systems permit such efficient reconstruction, given their far greater complexity. Remarkably, we demonstrate efficient and accurate prediction of disordered averaged QMI during long-time quench dynamics in the one-dimensional XXZ model with random field—across both many-body localized(MBL) and thermal phases—using only second-order correlations and a single universal nonlinear function trained on one Hamiltonian configuration, which can be readily adapted to predict the QMI across diverse experimental quantum platforms.

Model.— We study the dynamics of QMI following a sudden quench of duration t in the disordered XXZ model—a paradigmatic system for exploring many-body localization (MBL) [29]. The QMI, a highly non-local observable, is defined as

$$\delta S^{(n)} = S^{(n)}(\hat{\rho}_A) + S^{(n)}(\hat{\rho}_B) - S^{(n)}(\hat{\rho}),$$

for suitably chosen subsystems A and B. Here, $S^{(n)}(\hat{\rho}) = \log_2 \text{Tr} \hat{\rho}^n/(n-1)$ is the Rényi entropy (with integer n), and $\hat{\rho}_{A/B} = \text{Tr}_{B/A}[\hat{\rho}(t)]$ are reduced density matrices. The Hamil-

^{*} wpking@bnu.edu.cn

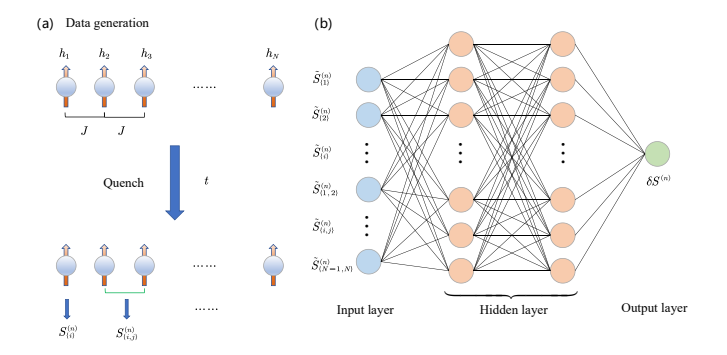


FIG. 1. The protocol to training the Rény entropy: a. The quenching dynamics of XXZ model and generation of local correlation and QMI for non-equilibrium state; **b**. The MLP method to learn the non-linear mapping between QMI $\delta S^{(n)}$ and local irreducible entropy $\delta S^{(n)}_i$, $\delta S^{(n)}_{\{i,j\}}$ with i,j be the index of the spins.

tonian of the XXZ chain is given by

$$\hat{H} = \sum_{i=1}^{N} h_i \hat{I}_{i,z} + \sum_{i=1}^{N-1} \left[\left(\hat{I}_{i,x} \hat{I}_{i+1,x} + \hat{I}_{i,y} \hat{I}_{i+1,y} \right) + J_z \hat{I}_{i,z} \hat{I}_{i+1,z} \right], \quad (1)$$

where $\hat{l}_{i,\alpha} = \hat{\sigma}_{i,\alpha}/2$ (with $i=1,\ldots,N$ and $\alpha=x,y,z$) is the spin operator at site i, and $\hat{\sigma}_{i,\alpha}$ are Pauli matrices. The disorder fields h_i are independent random variables uniformly distributed in [-W,W], and J_z controls the anisotropy. For $J_z=1$, the system undergoes an MBL-to-thermal transition at a critical disorder strength $W_c\approx 3.6$ [30, 31].

As illustrated in Fig. 1(a), we initialize the system in a random product state $|\Psi(0)\rangle = \bigotimes_{i=1}^N |m_i\rangle$, where $m_i \in \{+, -\}$ and $|\pm\rangle_i$ denote the eigenstates of $\hat{I}_{i,z}$. The state then evolves unitarily under the Hamiltonian (1) for a duration t. For the resulting state $|\Psi(t)\rangle = e^{-i\hat{H}t}|\Psi(0)\rangle$, we compute the QMI from the density matrix $\rho(t) = |\Psi(t)\rangle\langle\Psi(t)|$ for the chosen subsystems A and B.

We then employ the MLP to learn the relationship between the non-local QMI $\delta S^{(n)}$ and the local correlations (up to second order) of the non-equilibrium quantum state $|\Psi(t)\rangle$ generated by quenching dynamics described above. As is well known, the density matrix of the quantum state $|\Psi(t)\rangle$ can be fully described by the correlations $C_{\alpha_{i_1}}^{i_L}$ $\langle \Psi(t) | \prod_{n=1}^{L} \hat{\sigma}^{i_n}_{\alpha_{in}} | \Psi(t) \rangle$ of all the clusters, where L denotes the size of the cluster, $i_L = \{i_1, i_2, \dots, i_L\} (1 \le i_n \le N)$ is the index of spins, while $\alpha_{i_L} = \{\alpha_{i_1}, \alpha_{i_2}, \dots, \alpha_{i_L}\} (\alpha_{i_n} = x, y, z)$ is the collection of the spin indices. The total number of these correlations is $4^N - 1$. Measurement of these correlations is termed quantum state tomography(QST) and full access of these correlations can in principle give an exact reconstruction of the density matrix and hence the QMI $\delta S^{(n)}$. However, it is in fact impossible to measure all these correlations especially for quantum system with large size N due to exponentially increased measurement times. Consequently, it is highly desirable to investigate the relation between the OMI $\delta S^{(n)}$ and the local correlations up to the second order, which are easy to measure experimentally.

A central question is whether a universal relation exists be-

tween $\delta S^{(n)}$ and low-order correlations at arbitrary time t in the XXZ model. If such a function is found, it would enable experimental determination of the QMI $\delta S^{(n)}$ using only up to second-order local correlations, drastically reducing the measurement overhead required to reconstruct the QMI.

Method.—Before discussing the machine learning method, we first introduce the cluster correlation expansion method (CCE) for reconstructing the QMI inspired by methods for calculating decoherence [32, 33], as it provides physical insight into the underlying structure. Motivated by the gradual buildup of correlations during quenching dynamics, we can formally express the QMI as [see Supplemental Materials]

$$\delta S^{(n)} = -\sum_{L=2}^{N} \sum_{C_L} \tilde{S}_{C_L}^{(n)}, \tag{2}$$

where the sum runs over all connected clusters C_L of size L that intersect both subsystems A and B (i.e., $C_L \cap A \neq \emptyset$ and $C_L \cap B \neq \emptyset$). Clusters contained entirely within A or B do not contribute. Here, $\tilde{S}_{C_L}^{(n)}$ denotes the irreducible n-th Rényi entropy for cluster C_L , defined recursively via[32–34] [see supplementary materials]

$$\tilde{S}_{C_L}^{(n)} = S_{C_L}^{(n)} - \sum_{M=1}^{L-1} \sum_{C'_M \subset C_L} \tilde{S}_{C'_M}^{(n)}, \tag{3}$$

with the base case $\tilde{S}_{C_1}^{(n)} = S_{C_1}^{(n)}$, and where $S_{C_L}^{(n)} = \log_2 \text{Tr}[\rho_{C_L}^n]/(1-n)$ is the Rényi entropy of the reduced state on C_L . Each $S_{C_L}^{(n)}$ can be determined from correlations with order $\leq L$. Although Eq. (2) is exact, its evaluation requires high-order clusters, which becomes infeasible for large L. Alternately, we can truncate L to L_{\max} and make the approximation $\delta S^{(n)} \approx -\sum_{L=1}^{L_{\max}} \sum_{C_L} \tilde{S}_{C_L}^{(n)}$ (called CCE- L_{\max}) for short quenching time since the correlation is gradually built order by order and hence the genuine QMI of high order clusters should be very small for short quenching time. This truncation only requires lower order correlations with order $\leq L_{\max}$. The simplified case $L_{\max} = 2$ is the CCE-2 which only needs the first order expectation and second order correlations. However, these approximations obviously breaks down at longer times due to the proliferation of higher-order correlations.

Motivated by the CCE method, we want to ask whether the QMI can still be reconstructed by the 2-cluster correlation for long-time scale by machine learning, although the CCE-2 method fails in this case. This is because there may exist a nonlinear mapping between $\delta S^{(n)}$ and $\tilde{S}^{(n)}_{C_2}$ although the linear mapping fails based the on CCE-2 method in Eq. (2). The learning procedure is shown in Fig. 1. We first simulate the quenching quantum dynamics under the Hamiltonian \hat{H} in Eq. (1) for a certain random configuration h_i when the initial state is prepared as a random product state $|\Psi(0)\rangle = \bigotimes_{i=1}^N |m_i\rangle$. Then we calculate the QMI $\delta S^{(n)}$ and irreducible entropy $\tilde{S}^{(n)}_{C_L}$ based on the local correlations $C^{i_L}_{\alpha_{i_L}}(L \leq 2)$ for different quenching times t under various random configurations and random initial states, which is termed the training set. Finally, we use the generated irreducible Rényi entropy $\tilde{S}^{(n)}_{C_L}$ with $L \leq 2$ as the input of a multi-layer perceptron neural network

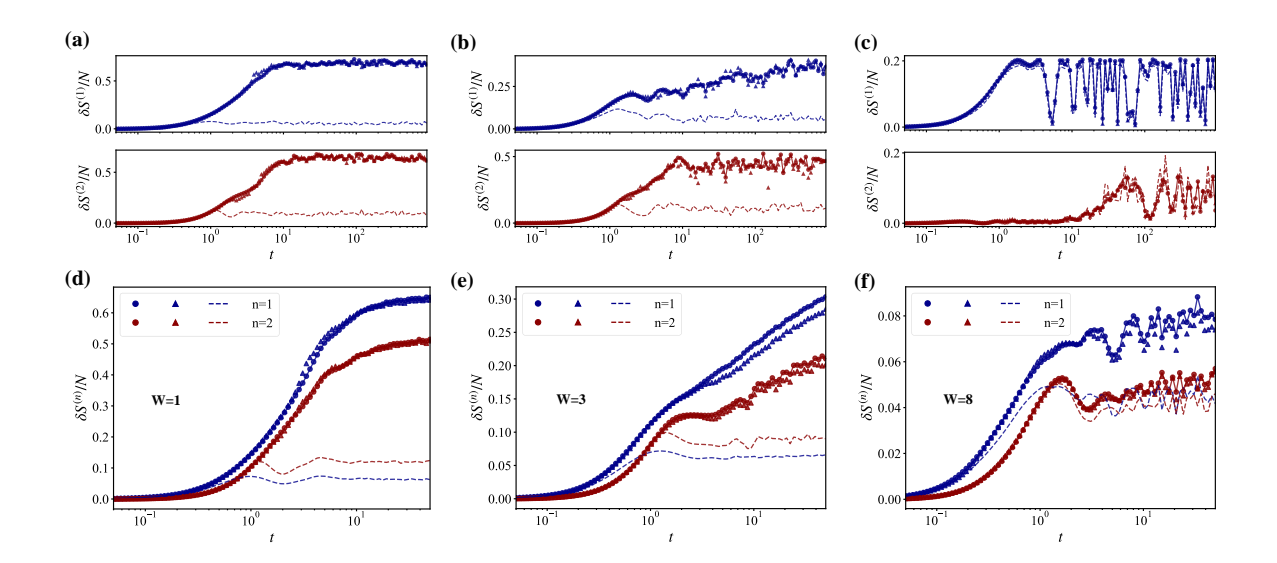


FIG. 2. **Machine learning of the dynamics of QMI** (a), (b), (c): The dynamics of QMI $\delta S^{(2)}/N$ of single disorder realization for different disorder strength: (a). W = 1, (b). W = 3, (c). W = 8 when fixing $J_z = 1$ and N = 10. $\delta S^{(2)}$ is calculated for the partitions $A = \{1, 2, 3, 4, 5\}$ and $B = \{6, 7, 8, 9, 10\}$. (d), (e), (f): The disorder averaged dynamics of $\delta S^{(n)}/N$ upper corresponding to the case (e), (d), (f). These results are obtained by averaging over 100 random disorder configuration. In all these figures, the circles, triangle and dashed line denotes the result that calculated by exact simulation, MLP and CCE method respectively.

to learn the nonlinear mapping to the QMI(see Fig. 1). Once the nonlinear mapping is trained, we use it to predict the QMI by the local correlations generated for random configurations and initial states totally different from the training set.

To train the QMI via local correlations by the method of MLP network, we implement a systematic deep learning framework. The activation function is chosen to be the Gaussian Error Linear Unit (GELU). This architecture was designed to capture the complex nonlinear mapping between the local correlations $\tilde{S}_{CL}^{(n)}(L \leq 2)$ and the QMI. To capture the broad distribution of QMI, we design a weighted hybrid loss function which balance overall accuracy and robustness in capturing weak signals[see Supplementary Materials].

Result.—First, we show that the MLP method precisely reconstructs the quenching dynamics of the QMI across a broad range of disorder strength. Since the maximum possible value of OMI is N, we predict the dynamics of $\delta S^{(n)}/N$ for disorder strengths W = 1, 3, 8 as shown in Fig. 2. Specifically, we take the initial state to be Neel states $|\Psi\rangle = |01010 \cdots 01\rangle$ without loss of generality[see supplementary materials for other initial states]. The upper panels[graph (a),(b), (c)] of Fig. 2 show results for a single disorder realization. For comparison, we also show the corresponding results calculated from CCE method. MLP method demonstrates obvious advantages over the CCE method. As shown by the curves in the upper panel of Fig. 2, CCE(dotted and dashed line) accurately captures $\delta S^{(n)}/N$ only at short times $t \ll 1$ or under strong disorder, whereas our method maintains accuracy across extended time scales ($\sim 10^9$) and all disorder strengths—particularly in the weak-disorder regime. This limitation of CCE originates from its perturbative nature, which restricts its validity to weakly correlated systems. As time increases beyond 1, correlations

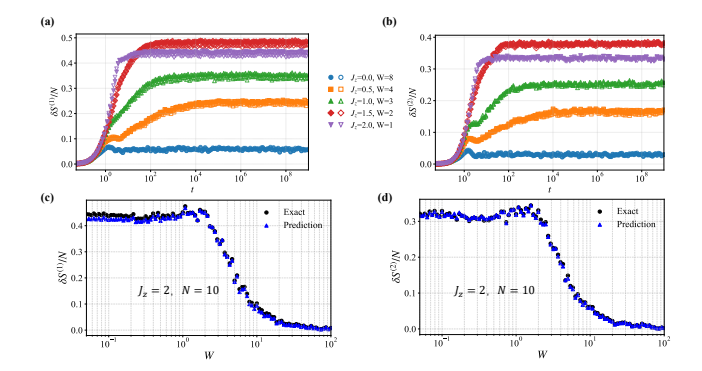


FIG. 3. Universal learning of the long-time dynamics of QMI: The prediction of long-time dynamics of QMI (a). $\delta S^{(1)}$; (b). $\delta S^{(2)}$ under different disorder strength W and anisotropy J_z using the universal model trained under the parameters $W=1,J_z=2$ and quenching time $t\in[0,200]$. In all these figures, the solid and empty scatters denotes the the result of exact simulation and prediction by MLP respectively. Different colors and shape denotes different parameters as shown in the legend of the graphs. (c) and (d) shows the prediction of long-time dynamics of QMI $\delta S^{(1)}$ and $\delta S^{(2)}$ respectively for fixed time $t=10^9$ and anisotropy $J_z=2$ as a function of disorder strength W using the universal model trained at the parameters $W=1,J_z=2$. The circle scatters and rectangle denotes the results from exact simulation and MLP respectively. The size of the system is taken to be N=10 and initial state to be Neel states.

propagate to higher orders, developing a nonperturbative character that renders CCE inadequate even at fourth order (CCE-4; see supplementary materials). Besides, it should also be emphasized that our model can predict $\delta S^{(n)}$ for different n(the case n = 1, 2 is demonstrated in Fig. 2) while the randomized

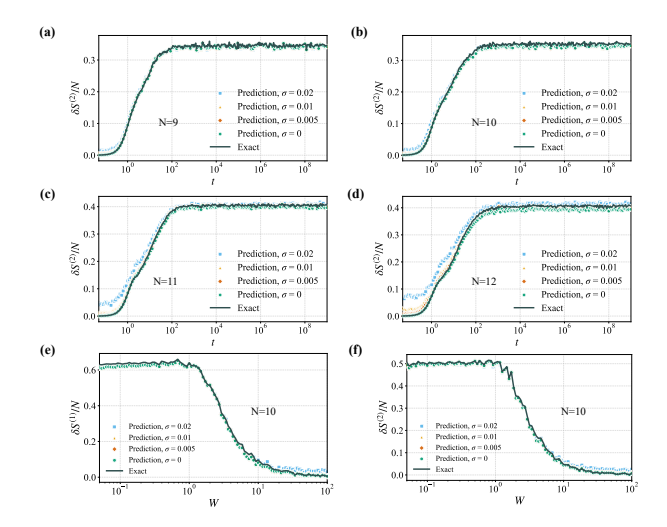


FIG. 4. **Robustness of the MLP method:** (a) N = 9, (b) N = 10, (c) N = 11 and N = 12: Machine learning of of long time dynamic of the QMI for different strength of the measurement noise and different system size; (e) and (f): Prediction of QMI $\delta S^{(1)}$ and $\delta S^{(2)}$ for fixed quenching time $t = 10^9$ as a function of disorder strength W under different noise strength σ . The size of the system is N = 10. All these prediction use the model trained at W = 1, $J_z = 1$.

measurements method in Ref. [16] can only predict the $\delta S^{(2)}$.

The observed tiny discrepancy between the MLP predictions and the exact simulation results can be attributed to two main factors. First, it may originate from the inherent limitations of the MLP approach based on correlations up to the second order. Improving the prediction accuracy would thus require the inclusion of even higher-order correlations. Second, the discrepancy could arise from the finite size of the training dataset. If this is the case, the accuracy should improve with more training samples. As shown in the Supplementary Material, we indeed find that the precision continues to increase with larger sample sizes. This suggests that the finite training data size is likely the dominant source of the discrepancy. Higher-order correlations could contribute, but their effect is likely most pronounced in capturing the fine features of the QMI dynamics.

For studying the MBL-thermal transition, disorderaveraged QMI is preferable as it reduces sample-to-sample fluctuations of random configurations [9]. We predict the QMI for individual disorder realizations and then average them over different configurations to obtain the disorder averaged QMI. Results in Fig. 2[lower panel, graphs (c),(d) and (e)] demonstrate that the MLP can still provide precise predictions of the disorder averaged QMI and offers more accurate predictions than that of single realization of disorder, since the configuration fluctuation is averaged. For W = 8 in Fig. 2(e) (MBL phase), the QMI exhibits slow initial growth followed by rapid oscillations, reflecting correlation propagation inhibited by strong disorder. The MLP results (blue triangle scatters) faithfully reproduce both the initial growth dynamics and the oscillatory features of exact calculations (blue circle scatters), as shown in Fig. 2 (c). For W = 1 in Fig. 2 (f)(thermal phase), as shown in Fig. 2 (a), $\delta S^{(n)}/N$ displays rapid initial growth followed by saturation at large values—behavior that our method can still capture accurately. At intermediate disorder (W=3), our approach also provides reliable predictions of the QMI dynamics, as evidenced in Fig. 2(d). These results clearly illustrate the non-perturbation nature of MLP methods.

Then we demonstrate the universality of our method for the prediction of the QMI $\delta S^{(n)}$. A universal model means that it can predict the dynamics of $\delta S^{(n)}$ generated under different parameters. It indicates that the different quantum states generated from different quenching process belong to the same complexity class. If this is true, once the model is trained, we can use a single model to predict the dynamics for other control parameters. This advantage will dramatically simplify the prediction process and reduce the time cost in realistic quantum quenching experiments.

To verify this, we investigate how to predict the long time(up to $t = 10^9$) dynamics of QMI $\delta S^{(n)}$ for a broad range of disorder strengths W based on the model trained from single parameters(W = 1 and $J_z = 2$). As shown in Fig. 3(a), (b), we plot the exact and predicted $\delta S^{(n)}$ for the case of n = 1, 2under the long time quenching process. We can see that the MLP model trained at $W = 1, J_z = 2$ can perfectly predict the long time dynamics of both $\delta S^{(1)}$ and $\delta S^{(2)}$ for W=1,2,3,4,8and $J_z \le 2$ from a single model trained in $W = 1, J_z = 2$. The reason that we choose to model at $W = 1, J_z = 2$ is that the model should possess enough complexity to encompass other cases. In summary, these results, in one aspect, show that the local second order correlations are enough to predict the complex quantum state even in the thermal phase $(W = 1, 2, 3 < W_c)$, where the QMI has scrambled to $\sim 0.6N$, a highly entanglement state which is usually expected to fail to describe by only second order correlations. In the other aspect, it implies an underlying similarity among these nonequilibrium quantum states, despite their preparation at different disorder strengths.

To show the power of the method, we also predict QMI at a fixed long-time scale $t = 10^9$ as a function of disorder strength W, whose performance has been previously used to identify critical phenomena near the many-body localization (MBL) transition [9]. Remarkably, this prediction is made despite the training data being restricted to the much shorter time interval $t \in [0, 200]$. As shown in Fig. 3(c,d), our model accurately captures the long-time behavior of $\delta S^{(n)}$ versus disorder strength, even though the local second-order correlations have completely evolved during this extended duration, which means the trained nonlinear function indeed captures the universal features of the complex state in one-dimensional XXZ model. This predictive power enables us to extract the critical point of the MBL-Thermal transition through the reconstruction of the QMI in quench dynamics and is particularly significant because conventional approaches require eigenstate properties that are experimentally inaccessible[35].

Finally, we examine the robustness of our prediction model against experimental measurement noise. In realistic settings, the noise in correlation measurements—determined by the number of measurement shots *M* and the signal-to-noise ratio (SNR)—introduces errors in the predicted QMI. To address

this, we add Gaussian noise with standard deviation σ to the expectation values and second-order correlations, and use the noisy data to predict the OMI. Since the noisy data would change the positivity of density matrix and hence be invalid to compute the inputs $\tilde{S}_{C_1}^{(n)}$ and $\tilde{S}_{C_2}^{(n)}$ of the MLP, we correct the noisy data via the optimization method shown in the Supplementary Materials. Using the corrected data, the prediction results are shown in Fig. 4. We observe that increasing the system size from N = 9 to N = 12 does not significantly degrade the prediction accuracy, suggesting that the trained model is robust to measurement noise, which remains accurate up to $\sigma \approx 0.01$. Based on the noise strength, we provide an estimation the possibility of experimental realization in different quantum platforms. By the central limit theorem, this noise level $\sigma \approx 0.01$ corresponds to a measurement budget of $M \approx 1/\sigma^2 \approx 10^4$ per second-order correlation, assuming perfect readout fidelity. The total number of measurements is then estimated as $9N(N-1)M/2 \approx 6 \times 10^6 (N \sim 12)$. In superconducting qubits, this corresponds to a total measurement time of approximately ~ 3 s for each time point and single configuration using the characteristic quenching time $10^2/J \sim 4\mu s[36](J)$ be the coupling strength of superconducting qubits) and a fast single-shot readout time of 100 ns in superconducting qubits system[37–39].

Conclusion and Discussion.—In this Letter, we introduce a machine learning framework based on MLP to efficiently predict the QMI in quench dynamics of the one-dimensional disordered XXZ spin chain, using only experimentally accessible second-order correlations and avoiding full quantum state tomography. Our approach successfully captures the non-equilibrium dynamics of the QMI across both many-body localized and thermalizing regimes.

Notably, the MLP-based method significantly outperforms conventional CCE techniques, especially at long times and in regimes of strong entanglement, where perturbative expansions break down. We further demonstrate the universality of the learned model: a network trained at a specific disorder

strength accurately predicts QMI dynamics over a wide range of disorders and times far beyond those seen during training. This suggests that the mapping from low-order correlations to non-local entropies exhibits a universal character across different dynamical phases. Moreover, the method proves robust to realistic measurement noise, indicating practical feasibility in experimental platforms such as superconducting qubits and ion traps with finite sampling resources.

Our results open a promising route toward the efficient and scalable characterization of non-local quantum information in many-body systems. More broadly, this data-driven approach illustrates how machine learning can uncover hidden universal relations between local observables and complex quantum properties in non-equilibrium dynamics, providing a powerful tool for studying quantum dynamics, phase transitions, and entanglement structures in regimes where traditional methods are intractable.

Future directions include extending the approach to higher dimensions and long-range interaction models, open quantum systems, other non-equilibrium dynamics, Fisher information, and out of time correlations[2], as well as combining it with advanced experimental techniques such as tensor networks[18], randomized measurements[16], or shadow tomography[25] to further enhance data efficiency.

Acknowledge.— P. W. is supported by the National Natural Science Foundation of China(Grant No. 12475012, Grant No. 62461160263), the Guangdong Provincial Quantum Science Strategic Initiative (Grant GDZX2403009, No. GDZX2303005) and the Quantum Science and Technology-National Science and Technology Major Project of China (Project 2023ZD0300600). H. L. is supported by the National Natural Science Foundation of China under Grant No. 62276171, the Guangdong Basic and Applied Basic Research Foundation, China, under Grant No. 2024A1515011938, and the Shenzhen Fundamental Research-General Project, China, under Grant No. JCYJ20240813141503005.

Supplementary Material

Detailed calculations, additional data figures, and methods are provided in the Supplementary Material [40].

^[1] N. Brunner, D. Cavalcanti, S. Pironio, V. Scarani, and S. Wehner, Bell nonlocality, Rev. Mod. Phys. **86**, 419 (2014).

^[2] A. G. J. MacFarlane, J. P. Dowling, and G. J. Milburn, Quantum technology: the second quantum revolution, Philosophical Transactions of the Royal Society of London. Series A: Mathematical, Physical and Engineering Sciences 361, 1655–1674 (2003).

^[3] O. Gühne and G. Tóth, Entanglement detection, Physics Reports 474, 1 (2009).

^[4] R. Islam, R. Ma, P. M. Preiss, M. Eric Tai, A. Lukin, M. Rispoli, and M. Greiner, Measuring entanglement entropy in a quantum many-body system, Nature 528, 77 (2015).

^[5] M. Heyl, Dynamical quantum phase transitions: a review, Reports on Progress in Physics 81, 054001 (2018).

^[6] N. Lambert, C. Emary, and T. Brandes, Entanglement and entropy in a spin-boson quantum phase transition, Phys. Rev. A 71, 053804 (2005).

^[7] J. Eisert, M. Friesdorf, and C. Gogolin, Quantum many-body systems out of equilibrium, Nature Physics 11, 124 (2015).

^[8] A. Nanduri, H. Kim, and D. A. Huse, Entanglement spreading in a many-body localized system, Phys. Rev. B 90, 064201 (2014).

^[9] R. Singh, J. H. Bardarson, and F. Pollmann, Signatures of the many-body localization transition in the dynamics of entanglement and bipartite fluctuations, New Journal of Physics 18, 023046 (2016).

^[10] A. M. Kaufman, M. E. Tai, A. Lukin, M. Rispoli, R. Schittko, P. M. Preiss, and M. Greiner, Quantum thermalization through entanglement in an isolated many-body system, Science 353, 794 (2016).

^[11] J. Venderley, V. Khemani, and E.-A. Kim, Machine learning out-of-equilibrium phases of matter, Physical review letters 120, 257204 (2018).

^[12] A. Lukin, M. Rispoli, R. Schittko, M. E. Tai, A. M. Kaufman,

- S. Choi, V. Khemani, J. Léonard, and M. Greiner, Probing entanglement in a many-body–localized system, Science **364**, 256 (2019).
- [13] C. Rovelli, Black hole entropy from loop quantum gravity, Phys. Rev. Lett. 77, 3288 (1996).
- [14] A. J. Daley, H. Pichler, J. Schachenmayer, and P. Zoller, Measuring entanglement growth in quench dynamics of bosons in an optical lattice, Phys. Rev. Lett. 109, 020505 (2012).
- [15] D. A. Abanin and E. Demler, Measuring entanglement entropy of a generic many-body system with a quantum switch, Phys. Rev. Lett. 109, 020504 (2012).
- [16] T. Brydges, A. Elben, P. Jurcevic, B. Vermersch, C. Maier, B. P. Lanyon, P. Zoller, R. Blatt, and C. F. Roos, Probing rényi entanglement entropy via randomized measurements, Science 364, 260 (2019).
- [17] A. Elben, R. Kueng, H.-Y. Huang, R. van Bijnen, C. Kokail, M. Dalmonte, P. Calabrese, B. Kraus, J. Preskill, P. Zoller, et al., Mixed-state entanglement from local randomized measurements, Physical Review Letters 125, 200501 (2020).
- [18] B. P. Lanyon, C. Maier, M. Holzäpfel, T. Baumgratz, C. Hempel, P. Jurcevic, I. Dhand, A. S. Buyskikh, A. J. Daley, M. Cramer, M. B. Plenio, R. Blatt, and C. F. Roos, Efficient tomography of a quantum many-body system, Nature Physics 13, 1158 (2017).
- [19] G. Carleo and M. Troyer, Solving the quantum many-body problem with artificial neural networks, Science 355, 602 (2017).
- [20] G. Torlai, G. Mazzola, J. Carrasquilla, M. Troyer, R. Melko, and G. Carleo, Neural-network quantum state tomography, Nature physics 14, 447 (2018).
- [21] J. Carrasquilla, G. Torlai, R. G. Melko, and L. Aolita, Reconstructing quantum states with generative models, Nature Machine Intelligence 1, 155 (2019).
- [22] M. Shin, J. Lee, and K. Jeong, Estimating quantum mutual information through a quantum neural network, Quantum Information Processing 23, 57 (2024).
- [23] M. Rieger, M. Reh, and M. Gärttner, Sample-efficient estimation of entanglement entropy through supervised learning, Physical Review A 109, 012403 (2024).
- [24] Y.-D. Wu, Y. Zhu, Y. Wang, and G. Chiribella, Learning quantum properties from short-range correlations using multi-task networks, Nature Communications 15, 8796 (2024).
- [25] H.-Y. Huang, R. Kueng, and J. Preskill, Predicting many properties of a quantum system from very few measurements, Nature Physics 16, 1050 (2020).
- [26] K. Xu, J.-J. Chen, Y. Zeng, Y.-R. Zhang, C. Song, W. Liu, Q. Guo, P. Zhang, D. Xu, H. Deng, et al., Emulating many-

- body localization with a superconducting quantum processor, Physical review letters **120**, 050507 (2018).
- [27] J. Chen, Z. Ji, Z. Wei, and B. Zeng, Correlations in excited states of local hamiltonians, Phys. Rev. A 85, 040303 (2012).
- [28] X.-L. Qi and D. Ranard, Determining a local Hamiltonian from a single eigenstate, Quantum 3, 159 (2019).
- [29] P. Sierant, M. Lewenstein, A. Scardicchio, L. Vidmar, and J. Zakrzewski, Many-body localization in the age of classical computing*, Reports on Progress in Physics 88, 026502 (2025).
- [30] D. J. Luitz, N. Laflorencie, and F. Alet, Many-body localization edge in the random-field heisenberg chain, Phys. Rev. B 91, 081103 (2015).
- [31] M. Serbyn, Z. Papić, and D. A. Abanin, Criterion for manybody localization-delocalization phase transition, Physical Review X 5, 041047 (2015).
- [32] W. Yang and R.-B. Liu, Quantum many-body theory of qubit decoherence in a finite-size spin bath, Phys. Rev. B 78, 085315 (2008).
- [33] W. Yang and R.-B. Liu, Quantum many-body theory of qubit decoherence in a finite-size spin bath. ii. ensemble dynamics, Phys. Rev. B 79, 115320 (2009).
- [34] M. Rispoli, A. Lukin, R. Schittko, S. Kim, M. E. Tai, J. Léonard, and M. Greiner, Quantum critical behaviour at the many-body localization transition, Nature 573, 385 (2019).
- [35] V. Khemani, S.-P. Lim, D. Sheng, and D. A. Huse, Critical properties of the many-body localization transition, Physical Review X 7, 021013 (2017).
- [36] M. Pita-Vidal, J. J. Wesdorp, L. J. Splitthoff, A. Bargerbos, Y. Liu, L. P. Kouwenhoven, and C. K. Andersen, Strong tunable coupling between two distant superconducting spin qubits, Nature Physics 20, 1158 (2024).
- [37] T. Walter, P. Kurpiers, S. Gasparinetti, P. Magnard, A. Potočnik, Y. Salathé, M. Pechal, M. Mondal, M. Oppliger, C. Eichler, and A. Wallraff, Rapid high-fidelity single-shot dispersive readout of superconducting qubits, Phys. Rev. Appl. 7, 054020 (2017).
- [38] Y. Sunada, S. Kono, J. Ilves, S. Tamate, T. Sugiyama, Y. Tabuchi, and Y. Nakamura, Fast readout and reset of a superconducting qubit coupled to a resonator with an intrinsic purcell filter, Phys. Rev. Appl. 17, 044016 (2022).
- [39] A. M. Gunyhó, S. Kundu, J. Ma, W. Liu, S. Niemelä, G. Catto, V. Vadimov, V. Vesterinen, P. Singh, Q. Chen, and M. Möttönen, Single-shot readout of a superconducting qubit using a thermal detector, Nature Electronics 7, 288 (2024).
- [40] X. H. Hao Liao and P. Wang, Supplementary material for "Universal learning of nonlocal entropy via local correlations in non-equilibrium quantum states" (2025).